Dynamic analysis of shells with the TRIC shell element

J. Argyris
Institute for Computer Applications
University of Stuttgart, D-70579 Stuttgart 80, Germany

M. Papadrakakis, Z. Mouroutis & A.G. Papachristidis
Institute of Structural Analysis & Seismic Research
National Technical University Athens, Zografou Campus, Athens 15780, Greece

ABSTRACT: In the present study the implementation of the natural mode method for finite element analysis is extended to the dynamic analysis of shell structures by formulating the kinematically consistent mass matrix of a model three-node multilayered triangular element (TRIC). Both translational and rotational inertia are included in the mass matrix which is generated using kinematic and geometric arguments consistent with the assumed natural rigid-body and straining modes of the element. Subsequently, numerical examples are performed to demonstrate the efficiency of the formulation and the potential of the natural mode method to deal efficiently with intricate time-dependent phenomena of shell structures.

Introduction

When faced with the challenge of investigating time-dependent nonlinear phenomena of shell structures with the finite element method a major constraint arises which is the high computational cost involved in the simulations. Higher order shell elements have been successfully proposed in the past for linear analysis. However, the extension of this type of shell elements to the nonlinear range and especially to time-dependent problems is not straightforward. Isoparametric finite elements based on higher-order interpolation functions and multiple quadrature loops can prove very expensive and cumbersome when applied to large and complex multilayered shells.

Hence, the development of a simple plate and shell finite element including transverse shear deformation, capable of engineering accuracy, competent in the study of intricate nonlinear phenomena and adaptable to many types of material systems including isotropic, sandwich, laminated, composite and hybrid structures remains a challenging task. A shell finite element that has been proved to have all the above-mentioned characteristics in static linear and nonlinear problems is the TRIC shell element Argyris et al. (1994).

The aim of this paper is to formulate a consistent mass matrix that includes both translational and rotational inertia in order to test the efficiency of the TRIC element in linear and nonlinear dynamic problems.

The mass matrix

The computation of the elemental mass matrix necesitates the estimation of matrix $\boldsymbol{\omega}$ containing the modal functions. More specifically, the displacement vector $\boldsymbol{u}$ must be expressed as a function of the natural modes. Then the global elemental mass matrix can be established via

$$\underset{(18x18)}{M_e} = \underset{(18x18)}{a^T}\left(\int_{V_e} \rho \underset{(18x3)}{\omega^T}\underset{(3x18)}{\omega}\, dV\right)\underset{(18x18)}{a} \qquad (1)$$

where $\boldsymbol{\alpha}$ is the transformation matrix from the local natural coordinate system of each element to the global Cartesian coordinate system and ρ is the density of the material.

The modal matrix $\boldsymbol{\omega}$ can be derived by invoking kinematic and geometric arguments. Similarly to static analysis, the rotational inertia forces resulting from antisymmetric deformation are assumed uncoupled from the other forces, and as such they are treated independently. The derivation of the part of the modal matrix that contains the rigid body modes is straightforward and it can be graphically depicted in Figure 1 Argyris et al. (1994).

The second component of the modal matrix is related to the axial straining modes ($\gamma_{t\alpha}$, $\gamma_{t\beta}$ and $\gamma_{t\gamma}$) along the sides of the triangular element. From Figure 2, it can be concluded that the displacements of node Γ, for example, is given by:

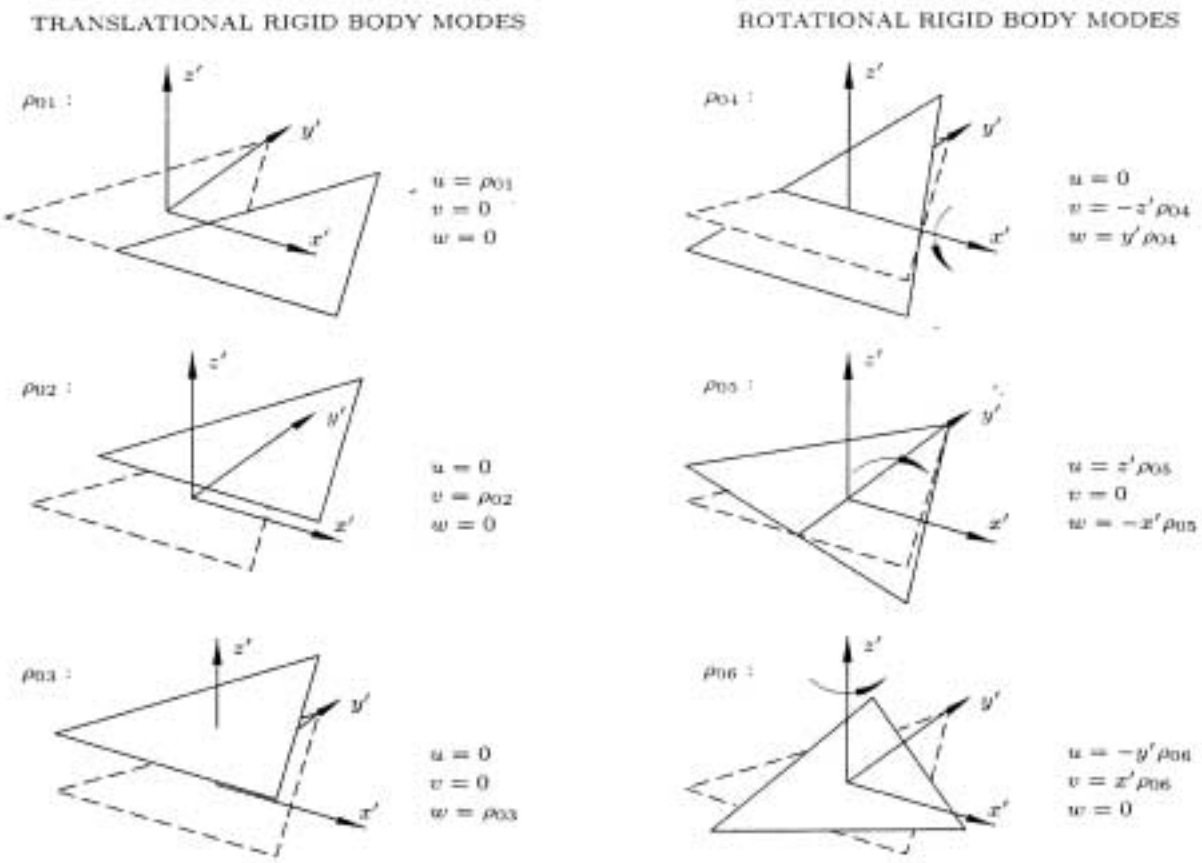

Figure 1

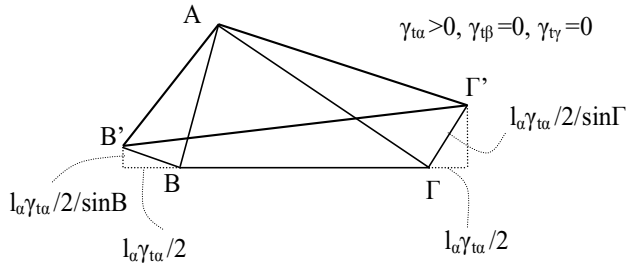

Figure 2

$$u_3 = \frac{l_a}{2\sin\Gamma}\cos\left(\beta-\frac{\pi}{2}\right)\gamma_{ta} + \frac{l_\beta}{2\sin\Gamma}\cos\left(a-\frac{\pi}{2}\right)\gamma_{t\beta} \tag{2}$$

$$v_3 = \frac{l_a}{2\sin\Gamma}\sin\left(\beta-\frac{\pi}{2}\right)\gamma_{ta} + \frac{l_\beta}{2\sin\Gamma}\sin\left(a-\frac{\pi}{2}\right)\gamma_{t\beta} \tag{3}$$

or:

$$u_3 = \frac{l_a\sin\beta}{2\sin\Gamma}\gamma_{ta} + \frac{l_\beta\sin\alpha}{2\sin\Gamma}\gamma_{t\beta} \tag{4}$$

$$v_3 = -\frac{l_a\cos\beta}{2\sin\Gamma}\gamma_{ta} - \frac{l_\beta\cos\alpha}{2\sin\Gamma}\gamma_{t\beta} \tag{5}$$

and finally:

$$u_3 = \frac{l_\alpha^2 l_\beta\sin\beta}{4\Omega}\gamma_{ta} + \frac{l_\alpha l_\beta^2\sin\alpha}{4\Omega}\gamma_{t\beta} \tag{6}$$

$$v_3 = -\frac{l_\alpha^2 l_\beta\cos\beta}{4\Omega}\gamma_{ta} - \frac{l_\alpha l_\beta^2\cos\alpha}{4\Omega}\gamma_{t\beta} \tag{7}$$

or:

$$u_3 = \frac{l_\alpha^2 y_\beta}{4\Omega}\gamma_{ta} + \frac{l_\beta^2 y_\alpha}{4\Omega}\gamma_{t\beta} \tag{8}$$

$$v_3 = -\frac{l_\alpha^2 x_\beta}{4\Omega}\gamma_{ta} - \frac{l_\beta^2 x_\alpha}{4\Omega}\gamma_{t\beta} \tag{9}$$

Similar expressions can be derived for the other two nodes leading to the following expressions for the inplane displacements of the element due to the axial straining modes along the side of the triangle:

$$u = \frac{l_\alpha^2}{4\Omega}\left(y_\gamma\zeta_\beta + y_\beta\zeta_\gamma\right)\gamma_{ta} + \frac{l_\beta^2}{4\Omega}\left(y_\alpha\zeta_\gamma + y_\gamma\zeta_\alpha\right)\gamma_{t\beta} + \frac{l_\gamma^2}{4\Omega}\left(y_\alpha\zeta_\beta + y_\beta\zeta_\alpha\right)\gamma_{t\gamma} \tag{10}$$

$$v = -\frac{l_\alpha^2}{4\Omega}\left(x_\gamma\zeta_\beta + x_\beta\zeta_\gamma\right)\gamma_{ta} - \frac{l_\beta^2}{4\Omega}\left(x_\alpha\zeta_\gamma + x_\gamma\zeta_\alpha\right)\gamma_{t\beta} - \frac{l_\gamma^2}{4\Omega}\left(x_\alpha\zeta_\beta + x_\beta\zeta_\alpha\right)\gamma_{t\gamma} \tag{11}$$

where ζ_α, ζ_β, ζ_γ, are the area coordinates of the triangular element.

By setting any of the axial straining modes equal to 1 and the others equal to zero the corresponding modal functions can be obtained.

For the derivation of the expressions of the symmetric and antisymmetric modal functions, the following expression of the vertical (out of the plane) displacement is used, Argyris et al. (2000):

$$w = \frac{1}{2}l_\alpha\zeta_\beta\zeta_\gamma\psi_{s\alpha} + \frac{1}{2}l_\beta\zeta_\alpha\zeta_\gamma\psi_{s\beta} + \frac{1}{2}l_\gamma\zeta_\alpha\zeta_\beta\psi_{s\gamma} + \frac{1}{2}l_\alpha\zeta_\beta\zeta_\gamma\left(\zeta_\beta - \zeta_\gamma\right)\psi_{A\alpha} + \frac{1}{2}l_\beta\zeta_\alpha\zeta_\gamma\left(\zeta_\gamma - \zeta_\alpha\right)\psi_{A\beta} + \frac{1}{2}l_\gamma\zeta_\alpha\zeta_\beta\left(\zeta_\alpha - \zeta_\beta\right)\psi_{A\gamma} \tag{12}$$

where $\psi_{s\alpha}$, $\psi_{s\beta}$ and $\psi_{s\gamma}$ are the natural symmetric bending modes and $\psi_{A\alpha}$, $\psi_{A\beta}$ and $\psi_{A\gamma}$ are the natural antisymmetric bending modes.

Thus, for example, for $\psi_{s\alpha}$=1 and all the other modes equal to 0 equation (12) becomes:

$$w = \frac{1}{2}l_\alpha\zeta_\beta\zeta_\gamma \tag{13}$$

Since:

$$u = -z\,\partial w/\partial x = -z\left(\frac{\partial w}{\partial\zeta_\alpha}\frac{\partial\zeta_\alpha}{\partial x} + \frac{\partial w}{\partial\zeta_\beta}\frac{\partial\zeta_\beta}{\partial x} + \frac{\partial w}{\partial\zeta_\gamma}\frac{\partial\zeta_\gamma}{\partial x}\right)$$
$$v = -z\,\partial w/\partial y = -z\left(\frac{\partial w}{\partial\zeta_\alpha}\frac{\partial\zeta_\alpha}{\partial y} + \frac{\partial w}{\partial\zeta_\beta}\frac{\partial\zeta_\beta}{\partial y} + \frac{\partial w}{\partial\zeta_\gamma}\frac{\partial\zeta_\gamma}{\partial y}\right) \tag{14}$$

the expressions for u, v become:

$$u = \frac{zl_\alpha}{4\Omega}\left(y_\beta\zeta_\gamma + y_\gamma\zeta_\beta\right)$$
$$v = -\frac{zl_\alpha}{4\Omega}\left(x_\beta\zeta_\gamma + x_\gamma\zeta_\beta\right) \tag{15}$$

In a similar way, the expressions of the other symmetric and antisymmetric modal functions can be deduced.

Finally, the expressions for the natural azimuth modes are graphically depicted in Figure 3, Argyris et al (1994).

Symbolic computation is employed in order to carry out, in a clear way, the tedious but otherwise straightforward matrix multiplications of Equation 1. Consequently, all integrals are evaluated in an exact manner using the formula:

$$\frac{1}{\Omega}\int_\Omega \zeta_a^p\zeta_\beta^q\zeta_\gamma^r d\Omega = \frac{2!\,p!q!r!}{(2+p+q+r)!} \tag{16}$$

The principle of virtual work in dynamics

The principle of virtual work for static (linear and nonlinear) in terms of the elastic Cartesian stresses and strains reads:

$$\int_V \sigma^{\mathrm{T}}\delta\varepsilon dV = \int_V p_V^T\delta u dV + \int_S p_S^T\delta u dV + R^T\delta r \tag{17}$$

where σ, ε denote the stress and elastic strain vectors, respectively; u is the displacement vector; p_V, p_S are the distributed body and distributed surface forces, respectively, and R is the vector of the concentrated forces or moments.

For dynamic analysis, the inertia and damping forces must be included in equation (17). The work produced by these forces can be written as:

$$W_I = \int_V u^T dR_I = r^T\int_V \rho\omega^T\omega dV\ddot{r} \tag{18}$$

$$W_D = \int_V u^T dR_D = r^T \int_V \mu \omega^T \omega dV \dot{r} \qquad (19)$$

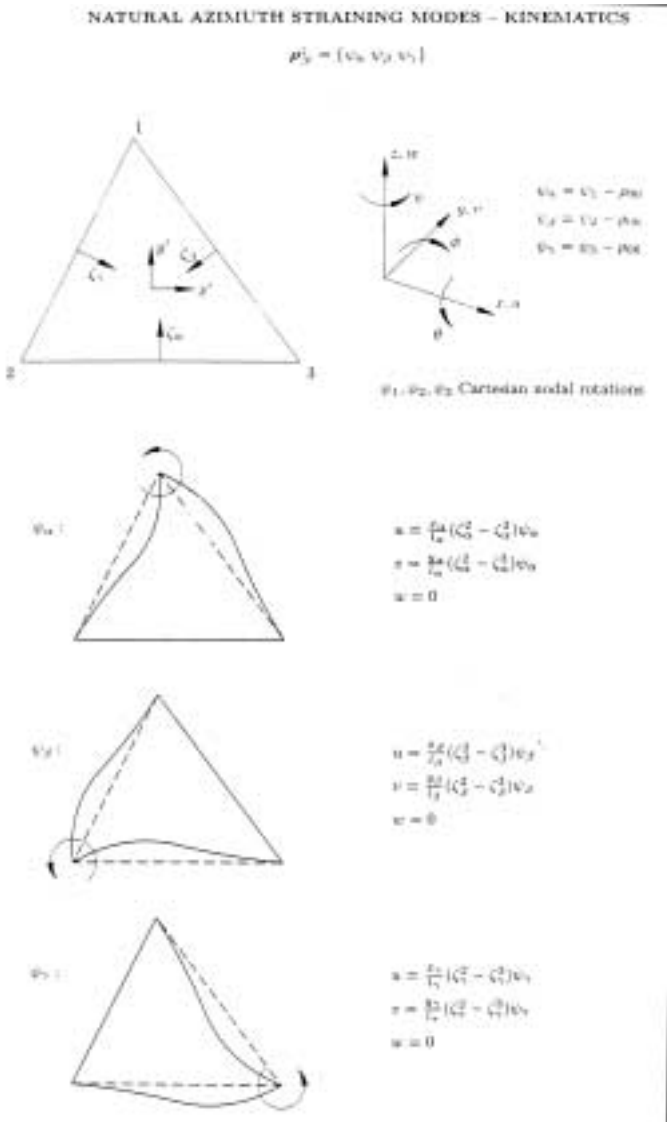

Figure 3

where μ is the local damping coefficient and $\boldsymbol{r}$ the vector of the nodal displacements.

Equation (17) modified with the introduction of the inertia and damping terms reads for a finite element e:

$$r^T(t)\left(\int_{V_e}\left[\left[\bar{\alpha}_{\mathrm{N}}\mathrm{T}_{06}\right]^{\mathrm{T}}\left[\alpha_{\mathrm{N}}^{\mathrm{T}}\kappa\alpha_{\mathrm{N}}\right]\left[\bar{\alpha}_{\mathrm{N}}\mathrm{T}_{06}\right]\right]_e dV\right) +$$
$$\ddot{r}^T(t)\left(\int_{V_e}\rho\omega^T\omega dV\right) + \dot{r}^T(t)\left(\int_{V_e}\mu\omega^T\omega dV\right) = \qquad (20)$$
$$\left(\int_{V_e} p(t)\omega^T\omega dV\right) + R_e^T(t)\delta r$$

or

$$K_e r(t) + M_e \ddot{r}(t) + C_e \dot{r}(t) = R_e(t) \qquad (21)$$

where K_e, M_e, C_e and $R_e(t)$ are the elemental stiffness, mass, damping matrices and the loading vector respectively.

Numerical examples

Numerical examples are presented to test and verify the proposed mass matrix derived for the TRIC shell element. The examples are linear dynamic problems. The results are compared to those produced by the commercial program SOFiSTiC for static and dynamic analysis of structures.

Plate with constant distributed load.

The first example examines the dynamic response of a plate which is fixed along one of its sides under a constant distributed vertical load.

The geometry of this shell example is shown in Figure 4

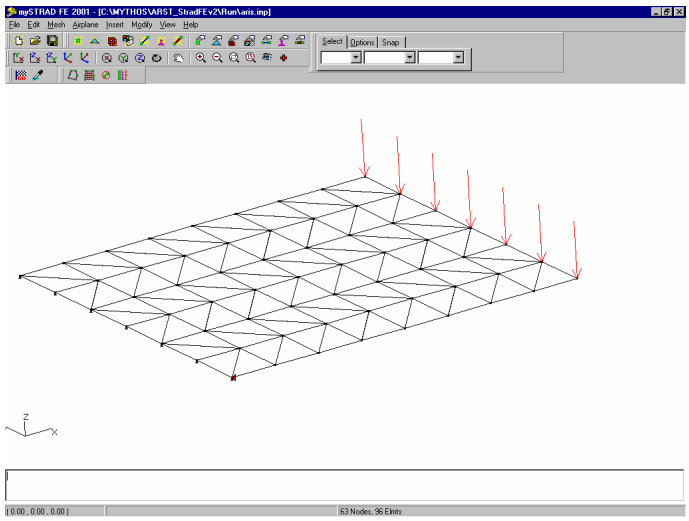

Figure 4

The width of this cantilever plate is 3m and the length is 4m. The thickness of the plate is considered to be 40cm. The modulus of elasticity is taken E=30000000kPa and the Poisson ratio equal to 0.2. The constant over time distributed load is equal to 40kN/m.

The plate is divided to 96 elements with 63 nodes as shown in Figure 4.

The results that were produced by the TRIC element are practically identical to those produced by the

SOFiSTiC program (see Figure 5) proving the accuracy of the proposed mass matrix formulation.

Plate with time dependent distributed load.
The same plate as in the previous example is solved with distributed load that diminishes linearly with time and becomes zero at time t=0.5sec.

The results are shown in Figure 6 and are again coincident to those produced by SOFiSTiC.

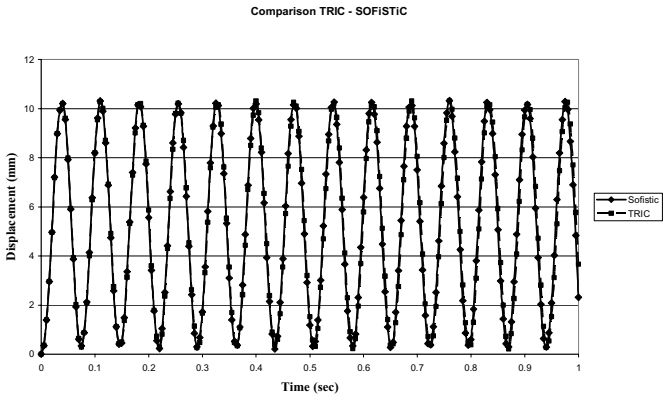

Figure 5

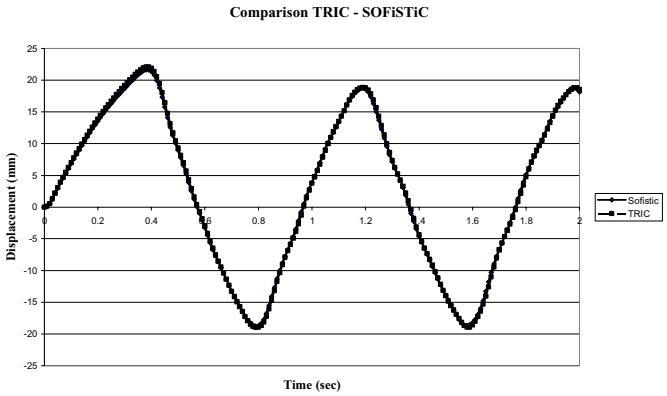

Figure 6

Shallow shell with concentrated load.
The next test example is a shallow shell with a concentrated load in the middle. Due to the symmetry of the structure along both axes only one quarter of the shell is examined (Figure 7). The concentrated load is equal to 1kN at time t=0 s and remains constant until time t=0.05 s when it becomes zero. The time step used is t=0.0005 s and the dynamic analysis is performed until time t=0.1 s. The results of the analysis are shown in Figure 8 where the performance of the TRIC element is compared with the quadrilateral shell elements of the commercial codes SOFiSTiC and NASTRAN. By comparing the results of the two commercial programs and the TRIC element it can be concluded that the results produced by the TRIC element are very satisfactory.

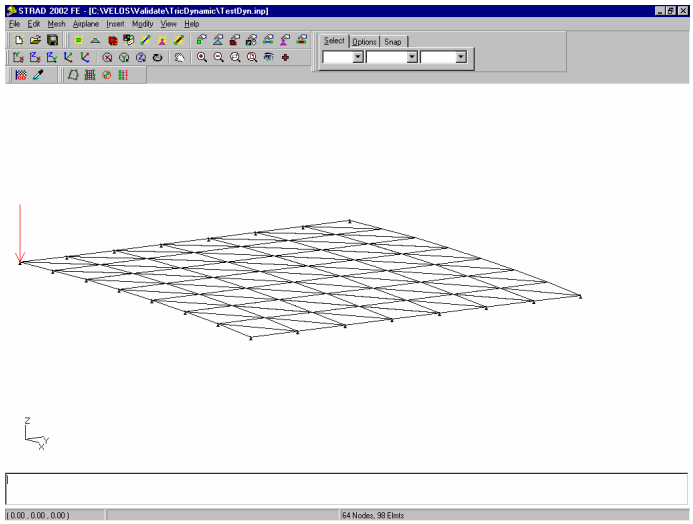

Figure 7

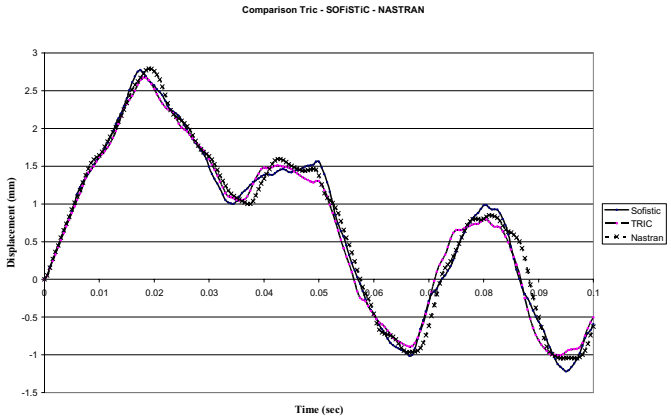

Figure 8

REFERENCES

J.H., Argyris, L. Tenek and L. Olofsson, “Nonlinear free vibrations of composite plates.” Comput. Methods Appl. Mech. Engrg., 115 (1994) 1-51.

J.H., Argyris, M. Papadrakakis, C. Apostolopoulou and S. Koutsourelakis, "The TRIC shell element: theoretical and numerical investigation." Comput. Methods Appl. Mech. Engrg., 182 (2000) 217-245.